46th AIAA/ASME/SAE/ASEE Joint Propulsion Conference & Exhibit
25 - 28 July 2010, Nashville, TN

AIAA 2010-7072

Pressure Variations in Rocket Nozzles. Part 1: Direct Asymptotic Predictions

Brian A. Maicke* and Joseph Majdalani†
University of Tennessee Space Institute, Tullahoma, TN 37388

We consider the one-dimensional flow equations that relate the expansion area ratio to the unique back pressures that define the operating modes of a nozzle. To eliminate guesswork and numerical root solving in deducing these unique threshold values, we apply asymptotic tools to invert their corresponding thermodynamic relations analytically. Our perturbation approach is based on the square of the reciprocal of the nozzle area expansion ratio, which does not exceed 0.3 in most applications. By extending our series approximation to higher orders, we develop a recursive expression that permits the efficient calculation of the pressure ratios to arbitrary levels of precision. In most cases, a three-term approximation entails an error of less than 1% for a nozzle expansion ratio up to 0.56. Furthermore, the error in these approximations slightly decreases as γ is decreased. All solutions are numerically verified and compared to tabulated values.

Nomenclature

A	=	local cross sectional area
A_t	=	nozzle throat area
a, b, m	=	coefficients given by Eq. (16)
p	=	normalized pressure, $\bar{p} / \bar{p}_c$
p_b	=	normalized back pressure, $\bar{p}_b / \bar{p}_c$
p_{opt}	=	normalized exit pressure at optimal expansion, $\bar{p}_{opt} / \bar{p}_c$
p_{sub}	=	normalized exit pressure at initial choking, $\bar{p}_{sub} / \bar{p}_c$
p_{sup}	=	normalized exit pressure with shock in the exit plane, $\bar{p}_{sup} / \bar{p}_c$
α	=	first constant in Eq. (6), $2/\gamma$
β	=	second constant in Eq. (6), $(\gamma+1)/\gamma$
ε	=	perturbation parameter, $(A_t / A_e)^2$
γ	=	ratio of specific heats
κ	=	exponent given by Eq. (15), $(\gamma-1)/(\gamma+1)$
ξ	=	constant related to γ via Eq. (4), $\kappa[\frac{1}{2}(\gamma+1)]^{\frac{2}{1-\gamma}}$

Subscripts and Symbols

0, 1	=	leading and first order
c	=	condition in the chamber
e	=	condition in the exit plane
n	=	asymptotic level
t	=	condition at the nozzle throat
$^-$	=	condition before a normal shock (minus)
$^+$	=	condition after a normal shock (plus)
$\bar{}$	=	overbars denote dimensional quantities

*Graduate Research Assistant, Mechanical, Aerospace and Biomedical Engineering Department. Member AIAA.
†H. H. Arnold Chair of Excellence in Advanced Propulsion, Mechanical, Aerospace and Biomedical Engineering Department. Senior Member AIAA. Fellow ASME.

I. Introduction

THE analysis of converging-diverging nozzle flows has long been of interest to both applied and theoretical researchers. After observing that a converging nozzle had limitations on the pressure ratios that it could achieve, Carl de Laval added a diverging section that greatly increased the efficiency and operating speed of the classical steam turbine.[1] Albeit a victory for turbine design, the earliest uses of the Laval nozzle did not have a firm theoretical basis. For example, choked flow was not considered and it was uncertain if the nozzle could promote supersonic flow conditions. These questions were later resolved in Stodola's landmark study in which he characterized the behavior of the flow through the nozzle, observing isentropic expansion and the existence of "compression shocks" in over-expanded nozzles.[2] Nozzle flow also intrigued Prandtl who augmented existing theory with his coverage of oblique shock and expansion fan phenomena, thus forming the bedrock of compressible flow theory.

While these classic studies provide a satisfying beginning, significant research on nozzles is currently underway. Modern applications abound especially in the areas of refrigeration,[3] mixing and entrainment,[4] flow metering,[5] cold powder spraying,[6,7] and propulsion.[8] To study the effects of nozzle cavitation, models for two phase flow analysis are implemented[9,10] while numerical simulations are used to quantify the effects of flow separation that can occur in rocket nozzles.[11] Of particular interest to turbomachinery applications are the effects of unsteady pressure fluctuations on shock formation.[12]

The practical applications of the Laval nozzle give rise to a set of fundamental challenges to the theoretical analyst. On the one hand, the flowfield is simple enough that it is often cast as a one-dimensional model. On the other hand, even with such an ambitious simplification, the resulting equations are often transcendental to the extent of disallowing direct analytical solutions. Indeed, modern textbooks still include compressible flow tables for handling one-dimensional nozzle expansions. Even the calculations for vital quantities, such as the nozzle back pressure, are carried out in multiple steps that require either interpolation of tabular data or iteration of numerical roots.

In fact, one-dimensional, isentropic flow theory offers two roots for the pressure ratio across a Laval nozzle. The subsonic root denotes the pressure ratio at which the throat first chokes, while the supersonic root corresponds to a fully flowing, supersonic nozzle with shock-free conditions. Between these two pressure ratios, isentropic solutions cannot exist and a non-isentropic process must be introduced. Evidently, a variety of agents can give rise to entropy increases. For example, both numerical simulations and experiments have shown that viscous effects can initiate oblique shocks, flow separation, recirculation, and expansion waves.[11] Because these effects require a departure from one-dimensional theory, an approximation can be made via a single normal shock introduced at some location in the nozzle.

Understanding these critical values is vital in understanding the effects of transients on nozzle performance. During start-up and shut down, the pressure in the chamber varies abruptly as the motor cycles up or blows down. The transient timescales are short, but significant sideloads can be incurred during transition through the over-expanded regime. Though asymmetries in the flow generally drive these sideloads, one-dimensional theory can provide the boundaries that separate the internal and external shock regions.

The aim of this study is to present closed form expressions for the critical back pressure ratios that separate the different regimes/modes of nozzle operation. Specifically, these regimes include subsonic, supersonic with internal shocks, supersonic with external shocks, and under-expanded supersonic flow. We exploit three basic relationships of one-dimensional compressible flow (i.e., Stodola's area ratio equation, the isentropic pressure equation, and the pressure ratio across a normal shock) to determine closed-form analytical expressions for three critical back pressures that delineate these regimes.

II. Mathematical Model

For our study we consider a nozzle, as shown in Fig. 1, with throat area A_t, exit area A_e and chamber pressure $\bar{p}_c$. The latter may be approximated with stagnation conditions owing to low velocities in the combustion chamber. We consider both a shock-free, isentropic nozzle and a nozzle containing a standing shock in the exit plane. For the standing shock case, we employ $\bar{p}^-$ and $\bar{p}^+$ to indicate the pressure before and after the shock, respectively.

To begin the exploration of the flow regimes in a Laval nozzle, we take a back pressure ratio larger than the subsonic root. In this case, the flow through the nozzle is entirely subsonic (see Fig 2a). For most applications, this situation is undesirable as it leads to the onset of a variable mass flow rate and a relatively modest flow energy. When the back pressure ratio is reduced to the first critical value, $p_{sub} = \bar{p}_{sub} / \bar{p}_c$, the flow at the throat becomes choked. Further reductions in the back pressure do not affect the flow upstream of the throat, and the mass flow rate through the nozzle remains constant. As the back pressure is further decreased, the flow behaves as in Fig 2b, accelerating after the throat until it reaches a standing normal shock inside the nozzle. This is a potentially hazardous area for propulsive applications as the flow in this range may lead to asymmetric separation which, in turn, can produce damaging sideloads inside the nozzle. Further reductions in the back pressure drive the standing shock wave toward the exit plane until the second critical value, $p_{sup} = \bar{p}_{sup} / \bar{p}_c$, is reached (see Fig. 2c) where the shock occurs in the nozzle exit plane. At this point, the flow within the nozzle is still entirely supersonic. With subsequent $\bar{p}_b$ reductions, the pressure in the exit plane drops below the actual back pressure.

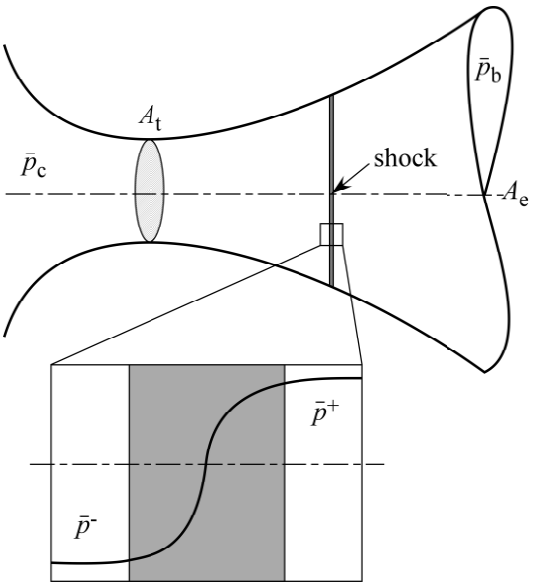

Figure 1. Schematic diagram of a nozzle hosting a normal shock.

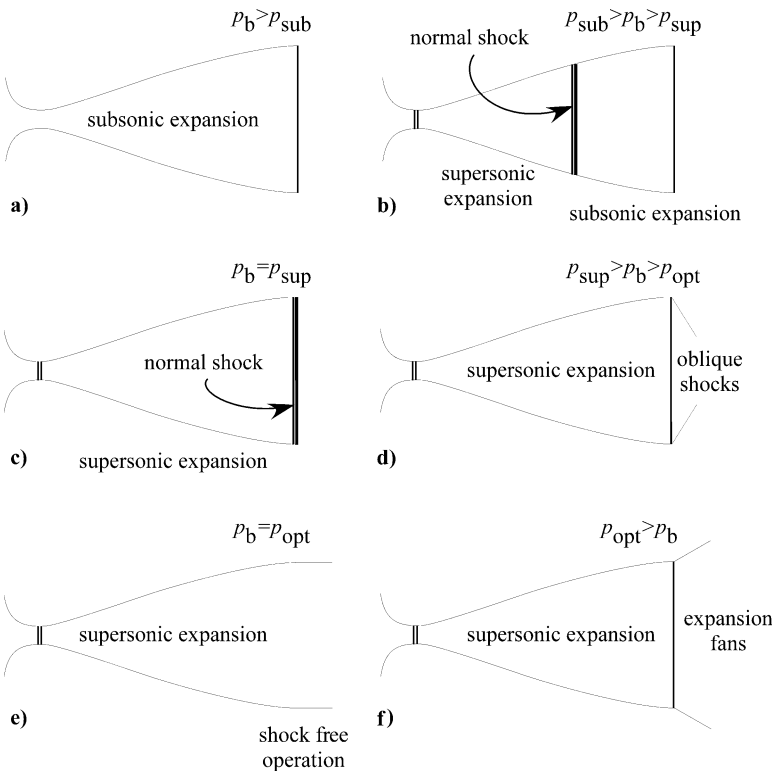

Figure 2. Modes of nozzle operation.

To compensate for this disparity, oblique shocks form at the edges of the nozzle as in Fig 2d. In this region the flow can no longer be handled with a one-dimensional model. Further decrements in the back pressure ratio will decrease the angle of the oblique shocks until isentropic supersonic shock-free operation is reached with $p_b = p_{opt}$ (see Fig. 2e). After this optimal expansion point is passed, the nozzle operates in an under-expanded mode. The increased pressure in the exit plane forces the formation of expansion fans, similar to those shown in Fig. 2f, through which the pressure is reduced to match the back pressure.

Two of these critical values are determined from a nonlinear relation connecting the nozzle area expansion ratio, $\varepsilon = \left(A_t / A_e\right)^2$, to the critical pressure ratio, $\bar{p}_b / \bar{p}_c$. This well-known expression takes the form[13]

$$\left(\frac{\bar{p}_b}{\bar{p}_c}\right)^{\frac{\gamma+1}{\gamma}}\left[\left(\frac{\bar{p}_b}{\bar{p}_c}\right)^{-\frac{\gamma-1}{\gamma}}-1\right]=\left(\frac{A_t}{A_e}\right)^2\left(\frac{\gamma-1}{\gamma+1}\right)\left(\frac{2}{\gamma+1}\right)^{\frac{2}{\gamma-1}} \tag{1}$$

Two roots precipitate from Eq. (1). The first, subsonic root, determines the largest back pressure $\bar{p}_{sub}$ that will still induce choked conditions at the throat. Further reductions in the back pressure do not affect conditions upstream of the nozzle; they only lead to further delays in oblique shock formation along the diverging sidewall of the nozzle. Shock effects lessen as we approach the second, supersonic root, often referred to as the optimal back pressure $\bar{p}_{opt}$ for a given nozzle area expansion ratio. Conversely, when $\bar{p}_{sub}$ is exceeded, sonic conditions at the throat become unattainable. Here $\bar{p}_c$ represents the chamber pressure approximated as the total stagnation pressure and $\gamma = c_p / c_v$ denotes the ratio of specific heats.

Equation (1) is applicable to a variety of propulsive applications involving variable area duct and nozzle flow. Due to its transcendental nature, however, it is traditionally inverted via numerical root solving. For this reason, numerical solutions rendering back pressure data versus nozzle area ratios are often presented in graphical or tabular form in several textbooks on the subject.[13-15] Equation (1) can apply to the entire flowfield within the nozzle and has been resolved analytically in a recent study of the isentropic pressure, density, and temperature in such a configuration.[16] However, when applied at the exit plane, the relationship determines the first and third critical points in the nozzle flowfield.

It is hence the purpose of this work to provide a unified analytical description of the flow through a converging-diverging nozzle including the necessary detail leading to a full analytical inversion of the missing critical pressure ratio for which a normal shock stands in the exit plane. This will be accomplished using asymptotic expansions that will enable us to express $\bar{p}_b$ as a direct function of $\bar{p}_c$, γ, and most importantly, A_t / A_e. The advent of a closed form expression for $\bar{p}_b$ will also enable us to calculate the pressure tolerance for a given nozzle by directly evaluating the ratio of $\bar{p}_b$ and the optimal expansion pressure $\bar{p}_e$.

III. Analysis

Before applying perturbation theory, we introduce the dimensionless back pressure $p_b = \bar{p}_b / \bar{p}_c$ and the small perturbation parameter $\varepsilon = \left(A_t / A_e\right)^2$. At the outset, Eq. (1) collapses into

$$p_b^{2/\gamma}\left(1-p_b^{1-1/\gamma}\right)=\varepsilon\left(\frac{\gamma-1}{\gamma+1}\right)\left(\frac{2}{\gamma+1}\right)^{\frac{2}{\gamma-1}} \tag{2}$$

Note that ε is the reciprocal of the square of the nozzle area expansion ratio. We make use of the relative size of ε which, according to Sutton,[17] varies customarily between 0.04 and 0.3. In actuality, ε can be as small as 0.0025 when involving high altitude nozzle applications. Such low values provide an

optimal environment for applying perturbation theory and retrieving a closed-form approximation for $p_b = p_b(\varepsilon, \gamma)$.

In what follows, we sketch the procedural steps needed to arrive at the desired solution. We also recognize that Eq. (2) exhibits two possible roots that correspond either to subsonic or supersonic exit conditions. The subsonic root will be first pursued to obtain the leading critical value, p_{sub}, the largest back pressure at which the nozzle chokes. As usual, results will be verified both theoretically and numerically.

A. Direct Isentropic Solutions for Threshold Pressures

To start, a regular perturbation approximation is invoked with ε at its epicenter. The dimensionless back pressure can be constructed from a series of diminishing terms, namely,

$$p_{sub}(\varepsilon, \gamma, n) = p_0 + \varepsilon p_1 + \varepsilon^2 p_2 + \ldots + \varepsilon^n p_n + O(\varepsilon^{n+1}) \tag{3}$$

where $p_{sub}(\varepsilon, \gamma, n)$ represents the solution at the nth order. Equation (2) may be further simplified into

$$p_{sub}^{2/\gamma} - p_{sub}^{1+1/\gamma} = \varepsilon\xi \text{ ; where } \xi \equiv \left(\frac{\gamma-1}{\gamma+1}\right)\left(\frac{2}{\gamma+1}\right)^{\frac{2}{\gamma-1}} \tag{4}$$

Further details of the solution can be found in a previous study by Majdalani and Maicke.[18] The total series solution is hence constructed and presented as

$$\begin{aligned} p_{sub} = 1 &- 2^{\frac{2}{\gamma-1}}\gamma(1+\gamma)^{\frac{1+\gamma}{1-\gamma}}\varepsilon - 3\gamma 2^{\frac{5-\gamma}{\gamma-1}}(1+\gamma)^{\frac{2(1+\gamma)}{1-\gamma}}\varepsilon^2 - \tfrac{5}{3}2^{\frac{7-\gamma}{\gamma-1}}\gamma(4+\gamma)(1+\gamma)^{\frac{3(1+\gamma)}{1-\gamma}}\varepsilon^3 \\ &- \tfrac{7}{3}2^{\frac{11-3\gamma}{\gamma-1}}\gamma(6+\gamma)(5+2\gamma)(1+\gamma)^{\frac{4(1+\gamma)}{1-\gamma}}\varepsilon^4 + O(\varepsilon^5) \end{aligned} \tag{5}$$

One can continue to higher orders until a repeatable trend is realized. This enables us to express the critical back pressure as a recursion capable of returning the solution to the nth order. We find[19]

$$\begin{aligned} p_{sub}(\varepsilon, \gamma, n) &= -\sum_{m=0}^{n} \frac{\prod_{j=1}^{m-1}\left[(m-j)\alpha + j\beta - 1\right]}{(-1)^{(2m)!}\, m!(\beta-\alpha)^m}(\varepsilon\xi)^m + O(\varepsilon^{n+1}) \\ &= 2 + \sum_{m=0}^{n} \frac{(-1)^{-(2m)!}(\varepsilon\xi)^m}{m!(\alpha-\beta)}\,\text{Pochhammer}\left[\frac{\alpha(1-m)-\beta+1}{\alpha-\beta}, m-1\right] + O(\varepsilon^{n+1}) \end{aligned} \tag{6}$$

where $\alpha \equiv 2/\gamma$ and $\beta \equiv (\gamma+1)/\gamma$. Similarly, the critical point for shock-free operation can be extracted from the same relation, though a different methodology is required to ensure convergence to the supersonic root. Instead of a regular perturbation, successive approximations are employed to determine the solution to the supersonic branch.

To determine the first order correction, we substitute $p_{opt} = p_0 + p_1$ into the pressure equation, factor out $p_0 = (\varepsilon\xi)^{\gamma/2}$, and employ a binomial expansion in p_1 / p_0. This operation results in

$$\begin{aligned} &p_0^{2/\gamma}\left[1 + (2/\gamma)(p_1/p_0) + O\left(p_1/p_0\right)^2\right] \\ &\quad - p_0^{(\gamma+1)/\gamma}\left[1 + (1+1/\gamma)\,p_1/p_0 + O\left(p_1/p_0\right)^2\right] - \varepsilon\xi = 0 \end{aligned} \tag{7}$$

whence

$$p_1 = \frac{p_0\left[p_0^{2/\gamma} - p_0^{(\gamma+1)/\gamma} - \varepsilon\xi\right]}{[(\gamma+1)/\gamma]p_0^{(\gamma+1)/\gamma} - (2/\gamma)p_0^{2/\gamma}} \tag{8}$$

In retaining additional terms, a recursive formulation can be found, namely,

$$p_m = \frac{\Pi_m^{2/\gamma} - \Pi_m^{(\gamma+1)/\gamma} - \varepsilon\xi}{\frac{\gamma+1}{\gamma}\Pi_m^{1/\gamma} - \frac{2}{\gamma}\Pi_m^{2/\gamma-1}}; \quad \Pi_m = \sum_{j=0}^{m-1} p_j; \qquad m \geq 1 \tag{9}$$

Since the total pressure is the summation of its constituents, we simply collect

$$p_{\text{opt}}(\varepsilon,\gamma,n) = (\varepsilon\xi)^{\frac{\gamma}{2}} + \sum_{m=1}^{n} p_m \tag{10}$$

The solutions in Eqs. (6) and (10) provide two of the three back pressure transition points during nozzle expansion. The third transition occurs when a deviation from isentropic behavior is considered, specifically when the flow passes through a normal shock.

B. Direct Non-Isentropic Solutions for Normal Shock Capture

The pressure ratio across a normal shock is given by the familiar relation

$$\frac{p^+}{p^-} = 1 + \frac{2\gamma}{\gamma+1}\left[(M^-)^2 - 1\right] \quad \text{or} \quad (M^-)^2 = \frac{1}{2\gamma}\left[\frac{p^+}{p^-}(\gamma+1) + \gamma - 1\right] \tag{11}$$

The pressure ratio p^+ / p^- for a normal shock standing in a nozzle can be determined as function of the area ratio by substituting the pre-shock Mach number into Stodola's equation, viz.

$$\left(\frac{A}{A_t}\right)^2 = \frac{1}{(M^-)^2}\left\{\frac{2}{\gamma+1}\left[1 + \frac{\gamma-1}{2}(M^-)^2\right]\right\}^{\frac{\gamma+1}{\gamma-1}} \tag{12}$$

The resulting expression becomes

$$(\gamma+1)\frac{p^+}{p^-} + \gamma - 1 = 2\varepsilon\gamma\left[\left(\frac{2}{\gamma+1}\right)\left\{1 + \frac{\gamma-1}{4\gamma}\left[(\gamma+1)\frac{p^+}{p^-} + \gamma - 1\right]\right\}\right]^{\frac{\gamma+1}{\gamma-1}} \tag{13}$$

The transcendental nature of Eq. (13) precludes a direct solution. However, using successive approximations, an accurate representation may be extracted. This is accomplished by first choosing $P = (\gamma+1)\,p^+ / p^- + \gamma - 1$ to the extent of reducing Eq. (13) into

$$P = 2\varepsilon\gamma\left[\left(\frac{2}{\gamma+1}\right)\left(1 + \frac{\gamma-1}{4\gamma}P\right)\right]^{\frac{\gamma+1}{\gamma-1}} \tag{14}$$

Equation (14) can be solved numerically for *P*. For values typical of nozzle applications, *P* is found to be a large quantity. This prompts us to set $X = 1/P$ and solve for *X* asymptotically. The *X* transformed relation becomes

$$X = (\varepsilon\gamma X)^{\kappa}(aX + b) \tag{15}$$

where

$$a \equiv 4^{\frac{\gamma}{\gamma+1}}\frac{\kappa}{\gamma-1}; \quad b \equiv 4^{-\frac{1}{\gamma+1}}\frac{\kappa}{\gamma}; \quad \kappa \equiv \frac{\gamma-1}{\gamma+1} \tag{16}$$

Assuming $X = X_0 + o(X_0)$ one gets, at leading order:

$$-(\varepsilon\gamma)^{\kappa} b X_0^{\kappa} + X_0 - (\varepsilon\gamma)^{\kappa} a X_0^{\kappa+1} = 0 \tag{17}$$

Realizing that $X_0 \ll 1$ and $\kappa < 1$, the last term may be ignored, being of higher order. This enables us to balance the first two members of Eq. (17) by setting

$$X_0 - (\varepsilon\gamma)^{\kappa} b X_0^{\kappa} = 0 \quad \text{or} \quad X_0 = b^{\frac{1}{1-\kappa}}(\varepsilon\gamma)^{\frac{\kappa}{1-\kappa}} = \frac{1}{2}\left[\frac{\gamma-1}{\gamma(\gamma+1)}\right]^{\frac{\gamma+1}{2}}(\varepsilon\gamma)^{\frac{\gamma-1}{2}} \tag{18}$$

Next, we let $X = X_0 + X_1 + o(X_1)$ and expand into

$$X_0 + X_1 - \left[\varepsilon\gamma\left(X_0 + X_1\right)\right]^{\kappa}\left[a\left(X_0 + X_1\right) + b\right] = 0 \tag{19}$$

Factoring out the leading term can be achieved by setting

$$X_0 + X_1 - \left(\varepsilon\gamma X_0\right)^{\kappa}\left(1 + \frac{X_1}{X_0}\right)^{\kappa}\left(aX_0 + aX_1 + b\right) = 0 \tag{20}$$

Recalling that $X_1 / X_0 << 1,$ a binomial expansion leaves us with

$$X_0 + X_1 - \left(\varepsilon\gamma X_0\right)^{\kappa}\left[1 + \kappa X_0^{-1}X_1 + \frac{\kappa(\kappa-1)}{2}X_0^{-2}X_1^2 + \ldots\right]\left(aX_0 + aX_1 + b\right) = 0 \tag{21}$$

To expedite matters, we neglect terms of $O\left(X_0^{-2}X_1^2\right)$ that entail smaller contributions. The resulting equation, when solved for X_1, produces

$$X_1 = \frac{\left(\varepsilon\gamma X_0\right)^{\kappa}(aX_0 + b) - X_0}{1 - \varepsilon^{\kappa}X_0^{\kappa}\left[a(\kappa+1) + b\kappa X_0^{-1}\right]} \tag{22}$$

The same method may be employed to generate higher-order approximations from the following recursive expression,

$$X = X_0 + \sum_{k=1}^{n} X_k; \quad X_k = \frac{\left(\varepsilon\gamma x_k\right)^{\kappa}(ax_k + b) - x_k}{1 - \varepsilon^{\kappa}x_k^{\kappa}\left[a(\kappa+1) + b\kappa x_k^{-1}\right]}; \quad x_k \equiv \sum_{j=0}^{k-1} X_j \tag{23}$$

To convert back to the laboratory coordinates, we use the direct expression

$$\frac{p^+}{p^-} = \frac{1}{(\gamma+1)X} - \kappa = \frac{1}{\gamma+1}\left[1 - \gamma + \left(X_0 + \sum_{k=1}^{n} X_k\right)^{-1}\right] \tag{24}$$

In order to compare Eq. (24) to the other threshold values, it is necessary to relate the solution to the chamber pressure. This can be easily accomplished by multiplying the result with the supersonic expansion relationship previously determined in Eq. (10). We readily obtain

$$\begin{aligned} p_{\text{sup}} &= \frac{p^+}{p^-}\frac{p^-}{p_{\text{c}}} = \frac{p^+}{p^-}p_{\text{opt}} \\ &= \frac{1}{\gamma+1}\left(1 - \gamma + \left\{\frac{1}{2}\left[\frac{\gamma-1}{\gamma(\gamma+1)}\right]^{\frac{\gamma+1}{2}}\left(\varepsilon\gamma\right)^{\frac{\gamma-1}{2}} + \sum_{k=1}^{n} X_k\right\}^{-1}\right)\left\{\left[\varepsilon\left(\frac{\gamma-1}{\gamma+1}\right)\left(\frac{2}{\gamma+1}\right)^{\frac{2}{\gamma-1}}\right]^{\frac{\gamma}{2}} + \sum_{m=1}^{n} p_m\right\} \end{aligned} \tag{25}$$

With Eqs. (6), (10), and (25) in hand, we can delineate the operational modes of a nozzle as the back pressure is reduced from stagnation to under-expanded conditions.

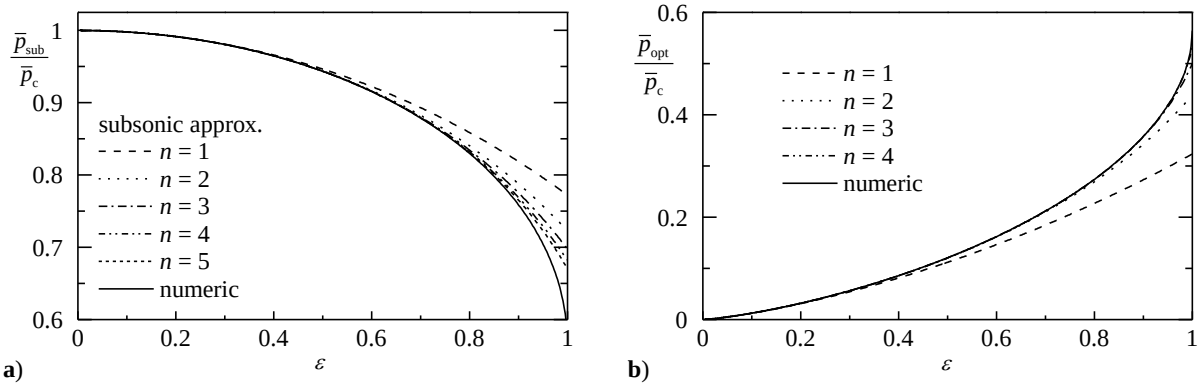

Figure 3. Comparison between numeric and asymptotic solutions for the threshold pressure ratios a) p_{sub} and b) p_{opt}.

IV. Results and Discussion

A detailed error analysis that pertains to Eqs. (6) and (10) can be found in Majdalani and Maicke.[18] For the reader's convenience we provide a graphical comparison of these results to the numerical solution of Eq. (2) in Fig. 3. The results appear to be in good agreement in the primary range of interest with slight deterioration as ε increases. Because of the recursive nature of solutions, an arbitrary level of precision can be reached through the inclusion of multiple terms, although a couple of terms only are sufficient for most applications.

To verify the efficacy of the shock pressure ratio calculation, we compare the values over a range of asymptotic orders with the numerical solution in Table 1. For the large expansion ratios common to most nozzle designs, the solution converges rapidly with only 3 terms and a relative error of less than 1%. The error is mildly dependent on γ as the solution displays decreasing absolute and relative errors when γ is varied from 1.6 to 1.2. Employing a realistic example, the space shuttle main engine has a nozzle area ratio of 77 that yields a value of 1.7×10^{-4} for ε. For $\gamma=1.4$, a simple *two-term* expansion provides a shock pressure ratio of 49.75 compared to a numerical value of 49.68, hence incurring a mere 0.14% discrepancy.

Having shown that the asymptotic form of the normal shock pressure ratio behaves properly, we use Fig. 4 to graphically reconcile the composite solution linking the back pressure ratio to the normal shock, as per Eq. (25). The approximations accommodate the numerical solution, with increasing deviations as the area ratio approaches unity. For propulsive applications, expansion ratios are invariably larger than 3, hence translating into $\varepsilon=0.11$ where a two-term approximation is adequate. This finding can be added to the subsonic and supersonic branches of Eq. (2) to produce a comprehensive map of nozzle operation through a range of back pressure values. Such a map can display the behavior of nozzle flow in four distinct regions.

Table 1. Verification of the asymptotic shock pressure ratio

		Number of terms for $\gamma=1.2$			
ε	Numeric	2	3	4	5
0.05	7.88	7.98	7.88	7.88	7.88
0.1	6.40	6.56	6.40	6.40	6.40
0.3	4.15	4.49	4.17	4.15	4.15
0.6	2.68	3.29	2.76	2.69	2.68
		Number of terms for $\gamma=1.6$			
ε	Numeric	2	3	4	5
0.05	14.57	14.79	14.58	14.57	14.57
0.1	10.68	10.94	10.70	10.68	10.68
0.3	5.84	6.23	5.90	5.85	5.85
0.6	3.34	3.94	3.48	3.37	3.35

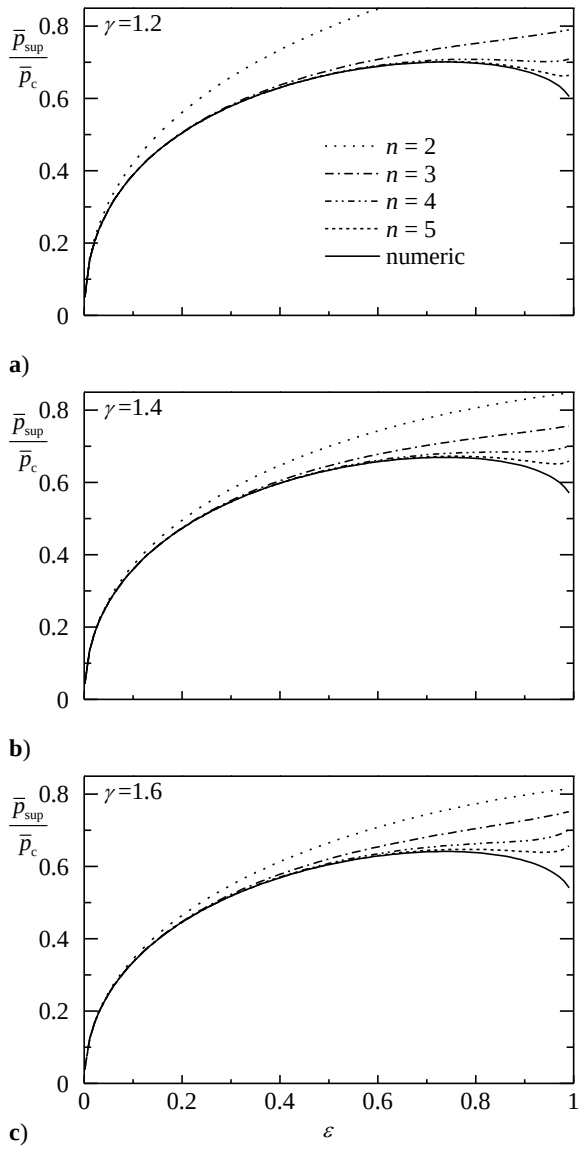

Figure 4. Numeric and asymptotic solutions of the supersonic back pressure using γ= a) 1.2, b) 1.4 and c) 1.6.

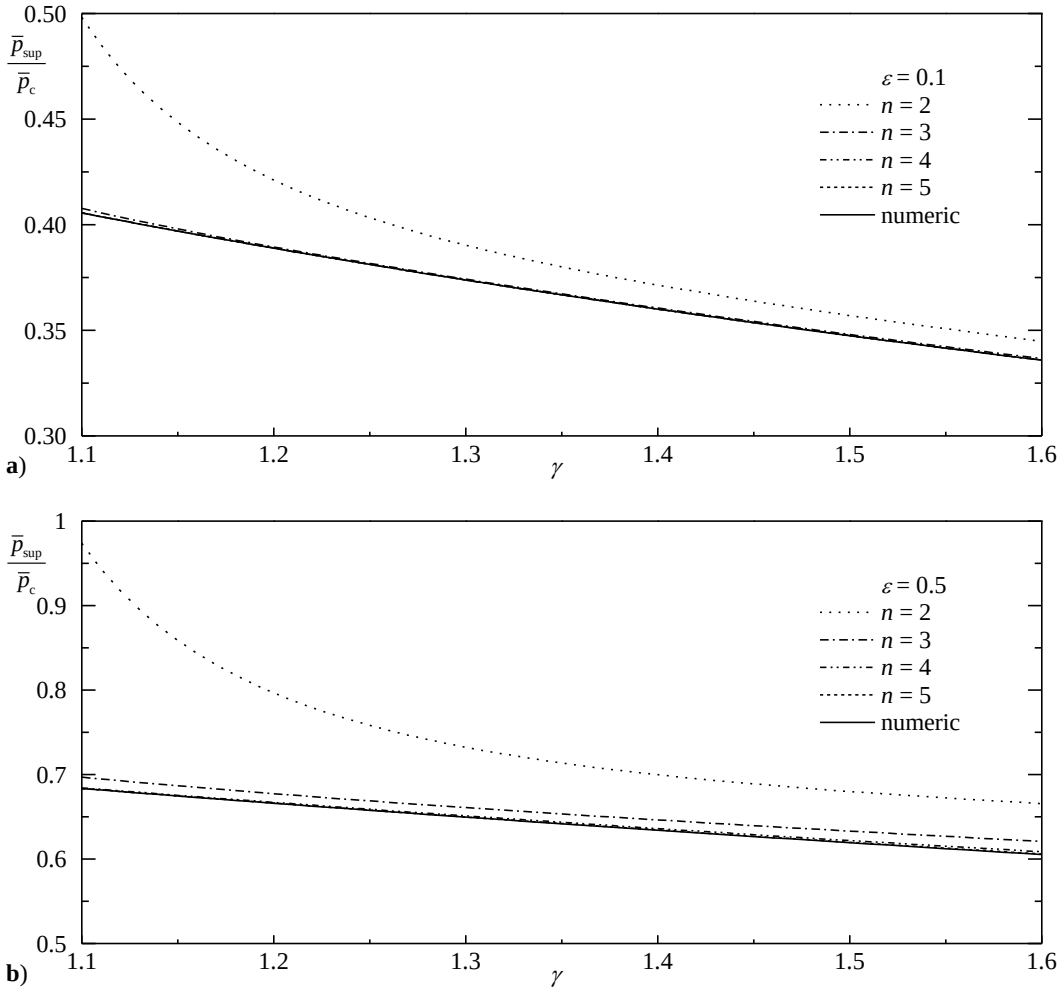

Figure 5. Variations in the supersonic back pressure ratio p_{sup} for a) ε = 0.1 and b) 0.5.

The construction of the map and a discussion of its benefits and limitations will be presented in Part 2 of this paper series.[20] In one of the regions, the flow throughout the nozzle will be subsonic. In the second region, the flow will exhibit normal shocks at some intermediate location between the throat and nozzle exit plane.

As the pressure drops below the supersonic threshold pressure, $p_b < p_{sup}$, the shock begins to bow out from the nozzle exit plane as shown in Fig. 2d. Oblique shocks begin to form and one-dimensional theory no longer provides an accurate assessment of the flowfield. The nozzle will be under-expanded and expansion fans occur in the exit plane as the relatively higher pressure exhaust tries to merge with the surrounding gas. It is interesting to note that the relative size of the operation modes is not constant. A more detailed discussion of the ensuing physical mechanisms is given in the companion paper.[20] As for the effect of γ itself, its variations are captured in Fig. 5. Therein, the supersonic back pressure ratio is described over the entire range of γ and two values of the area-Mach number squared. The horizontal axis represents γ and the curves are shown at constant values of a) $\varepsilon = 0.01$ and b) 0.5. For the range of normal motor operation, increasing the compression ratio leads to an almost linear decrease in the supersonic pressure ratio as clearly displayed in Fig. 5.

V. Concluding Remarks

This study focuses on the one-dimensional flow relations that relate the expansion area ratio to the critical back pressures that delineate the different operational modes of a converging-diverging nozzle. As we seek to eliminate guesswork and numerical root solving in deducing these threshold values, we apply asymptotic tools to the extent of inverting the corresponding thermodynamic relations analytically. To the authors' knowledge, the resulting closed-form solutions represent novel additions to the compressible flow literature. Our perturbation approach, being reliant on the reciprocal of the nozzle area expansion ratio, provides a proper approximation. By extending our series to higher orders, we unravel simple recursive expressions that permit the efficient calculation of the pressure ratio to arbitrary levels of precision. Favorable correspondence with the numerical solution at several gas compression ratios is also achieved as the relative error in a three-term approximation is found to drop, for example, below 0.57% for a nozzle area ratio of 0.3 and γ = 1.2. The error slightly decreases as the gas compression ratio is increased. Then using an explicit relation for the exit pressure, the pressure ratio for the supersonic back pressure is obtained analytically as a direct function of the area ratio and γ. In concert with the solution for p_{sup}, we present an explicit solution for the isentropic pressure relation, providing p_{sub} and p_{opt} boundaries for a given nozzle expansion area ratio.

By expressing the critical back pressures in terms of the nozzle area expansion ratio, we have provided a simple and direct analytical avenue to calculate these fundamental thermodynamic properties. Our asymptotic solutions are extended to arbitrary order to the extent of becoming applicable anywhere within a nozzle, including sections adjacent to the throat where the area ratio approaches unity. These formulations increase our repertoire of isentropic flow expressions that are widely used in the propulsion community. It is hoped that their development will aid in achieving direct solutions in several related nozzle flow investigations, including a treatment of the blowdown mechanism that arises at the end of a mission as the combustion chamber depressurizes.

Acknowledgments

This work was completed with the support of the National Science Foundation through Grant No. CMMI-0928762.

References

[1]Anderson, J. D., *Modern Compressible Flow with Historical Perspective*, 3rd ed., McGraw-Hill, New York, 2003.

[2]Stodola, A., *Steam Turbines*, Springer-Verlag, Berlin, 1903.

[3]Chunnanond, K., and Aphornratana, S., "An Experimental Investigation of a Steam Injector Refrigerator: The Analysis of the Pressure Profile Along the Ejector," *Applied Thermal Engineering*, Vol. 24, 2004, pp. 311-322. doi: 10.1016/j.applthermaleng.2003.07.003

[4]Raman, G., and Taghavi, R., "Resonant Interaction of a Linear Array of Supersonic Rectangular Jets: An Experimental Study," *Journal of Fluid Mechanics*, Vol. 309, 1996, pp. 93-111. doi: 10.1017/S0022112096001577

[5]Park, K. A., Choi, Y. M., Choi, H. M., Cha, T. S., and Yoon, B. H., "The Evaluation of Critical Pressure Ratios of Sonic Nozzles at Low Reynolds Numbers," *Flow Measurement and Instrumentation*, Vol. 12, 2001, pp. 37-41. doi: 10.1016/S0955-5986(00)00040-6

[6]Dykhuizen, R. C., and Smith, M. F., "Gas Dynamic Principles of Cold Spray," *Journal of Thermal Spray Technology*, Vol. 7, No. 2, 1998, pp. 205-212. doi: 10.1361/105996398770350945

[7]Jodoin, B., "Cold Spray Nozzle Mach Number Limitation," *Journal of Thermal Spray Technology*, Vol. 11, No. 4, 2002, pp. 496-507. doi: 10.1361/105996302770348628

[8]Hagemann, G., Immich, H., Nguyen, T., and Dumnov, G., "Advanced Rocket Nozzles," *Journal of Propulsion and Power,* Vol. 14, No. 5, 1998, pp. 620-634. doi: 10.2514/2.5354

[9]Preston, A. T., Colonius, T., and Brennen, C. E., "A Numerical Investigation of Unsteady Bubbly Cavitating Nozzle Flows," *Physics of Fluids,* Vol. 14, No. 1, 2002, pp. 300-311. doi: 10.1063/1.1416497

[10]Wang, Y. C., and Brennen, C. E., "One-Dimensional Bubbly Cavitating Flows through a Converging-Diverging Nozzle," *Journal of Fluids Engineering,* Vol. 120, 1998, pp. 166-170. doi: 10.1115/1.2819642

[11]Frey, M., and Hagemann, G., "Restricted Shock Separation in Rocket Nozzles," *Journal of Propulsion and Power,* Vol. 16, No. 3, 2000, pp. 478-484. doi: 10.2514/2.5593

[12]Gerolymos, G. A., and Bréus, J. P., "Computation of Unsteady Nozzle Flow Resulting from Fluctuating Back-Pressure Using Euler Equations," *Aerospace Science and Technology,* Vol. 2, No. 2, 1996, pp. 91-105. doi: 10.1016/S0034-1223(98)80008-0

[13]Oosthuizen, P. H., and Carscallen, W. E., *Compressible Fluid Flow*, McGraw-Hill, New York, 1997.

[14]Moran, M. J., and Shapiro, H. N., *Fundamentals of Engineering Thermodynamics*, 5th ed., John Wiley, New York, 2004.

[15]Çengel, Y. A., and Boles, M. A., *Thermodynamics: An Engineering Approach*, 4th ed., McGraw-Hill, New York, 2002.

[16]Majdalani, J., and Abu-Irshaid, E. M., "General Solutions for Some Isentropic Equations in Variable Area Duct Flow," AIAA Paper 2005-4382, July 2005.

[17]Sutton, G. P., *Rocket Propulsion Elements*, 6th ed., John Wiley, New York, 1992.

[18]Friedrich, M. A., Lan, H., Wegener, J. L., Drallmeier, J. A., and Armaly, B. F., "A Seperation Criterion with Experimental Validation for Shear-Driven Films in Seperated Flows," *Journal of Fluids Engineering,* Vol. 130, No. 5, 2008, pp. 051301-9. doi: 10.1115/1.2907405

[19]Majdalani, J., and Maicke, B. A., "Inversion of the Fundamental Isentropic Expansion Equations in Variable Area Duct Flow," AIAA Paper 2010-4861, June 2010.

[20]Maicke, B. A., Majdalani, J., and Geisler, R. L., "Pressure Variations in Rocket Nozzles. Part 2: Analytical Predictions During Blowdown," AIAA Paper 2010-7073, July 2010.